

Ultralow drift in organic thin-film transistor chemical sensors by pulsed gating

Richard D. Yang and Jeongwon Park

Materials Science and Engineering Program, University of California, San Diego, La Jolla, California 92093

Corneliu N. Colesniuc and Ivan K. Schuller

Department of Physics, University of California, San Diego, La Jolla, California 92093

William C. Trogler and Andrew C. Kummel^{a)}

Department of Chemistry and Biochemistry, University of California, San Diego, La Jolla, California 92093

(Received 7 May 2007; accepted 25 June 2007; published online 15 August 2007)

A pulsed gating method has been developed to enhance the baseline stability of organic thin-film transistor (OTFT) chemical sensors. Trap states in the organic films are the major source of the OTFTs baseline drift under static gate bias, which is identified as the bias stress effect (BSE). BSE typically reduces the baseline current by 60% over 20 h in phthalocyanine based OTFT sensors. The baseline drift has been reduced below 1% over 20 h in the absence of the analyte using the pulsed gating method. With pulsed gating, the baseline drift on exposure to 15 methanol pulses is less than 0.09% /h, and the response to this analyte is fully recoverable. Similar ultralow drift results were obtained for methanol sensing on three different phthalocyanine OTFTs. Combining the pulsed gating with low duty cycle analyte pulses, this method is also applicable to obtain ultralow drift (0.04% /h) even for low vapor pressure analytes such as organophosphonate nerve agent simulants.

© 2007 American Institute of Physics. [DOI: [10.1063/1.2767633](https://doi.org/10.1063/1.2767633)]

I. INTRODUCTION

Organic thin-film transistors (OTFTs) have been investigated for chemical vapor sensing since 2000.¹ These devices represent one recent type of chemically sensitive field-effect transistors (ChemFETs). In some earlier forms of ChemFETs, the organic films were deposited on top of the silicon metal oxide semiconductor field effect transistor (MOSFET) gate electrodes for sensing.² Conversely, in the present ChemFET devices, the organic films are the channel materials and are directly conducting the charge carriers. ChemFETs with channels of small organic molecules^{1,3-6} or conducting polymers^{7,8} show high sensitivity and selectivity to a range of gas vapors. It has been demonstrated that ChemFETs reach part per billion (ppb) level sensitivity to volatile organic vapors,³ ozone,⁹ and explosive agent simulants.¹⁰ The ChemFET response has also been shown to be tunable by changing the functional groups of organic materials, thereby making these sensors appealing for electronic nose (e-nose) application.^{7,8} In an e-nose, chemical responses acquired from an array of chemical sensors are used for pattern recognition.¹¹ E-noses can identify complex odors, but are especially sensitive to baseline drift and have to be frequently recalibrated.¹² While reference sensors or complicated drift compensation algorithms are often used to reduce the drift effect,¹¹ e-nose systems can be greatly enhanced by using low drift sensing techniques. Despite many studies of the chemical sensitivity of OTFT sensors,¹⁻⁸ the baseline stability of these sensors is still an issue.^{13,14}

The sources of baseline instability in ChemFETs include electrical, thermal, and analyte-induced instabilities. For OTFTs, the electrical instability is usually the major cause of the baseline drift. With static gate bias operation, even encapsulated OTFTs exhibit a large bias stress effect (BSE).¹⁵ This bias instability has been observed in OTFTs fabricated with a wide range of active materials, i.e., pentacene¹⁵ and thiophene derivatives,¹⁶ and is associated with charge trapping in the organic films. The trap states are energetically favorable for localizing charge carriers. The charge carriers are most stable in the trap states, but eventually become thermally excited and are released to either the valence (holes) or conduction (electrons) bands. The thermal instability of OTFTs is governed by the thermally activated charge transport properties of organic thin films,¹⁷⁻¹⁹ and can be mitigated by stabilizing the device temperature. The analyte-induced drift of ChemFETs has been found to depend on film thickness, which can be minimized by employing ultrathin channel materials.¹⁰

The electrical instability of organic materials impairs sensing applications of OTFTs, including chemical¹⁰ and thermal sensing.²⁰ A time delay over 300 s between consecutive current measurements has been shown to circumvent the BSE problem in thermal sensing.²⁰ However, a time delay is disruptive for chemical sensing applications, which often require continuous monitoring of the sensor output. A number of groups have investigated the BSE in OTFTs and shown that BSE is reversible after either long relaxation, reverse gate biasing, or photoillumination,²¹ suggesting that BSE is an electronic phenomenon rather than a physical degradation of devices.²² Organic thin films are known to contain a high

^{a)}Electronic mail: akummel@ucsd.edu

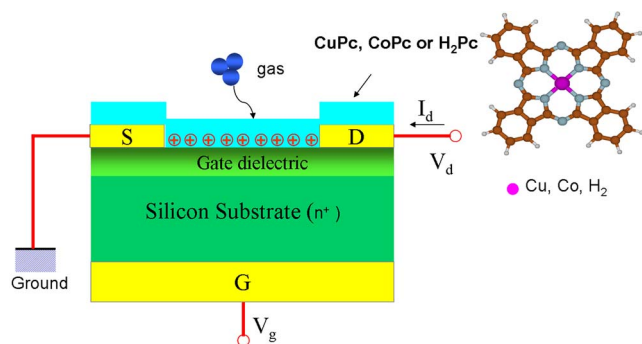


FIG. 1. (Color online) Cross section of a ChemFET. A 5 nm Ti adhesion layer and 45 nm thick gold source (S) and drain (D) pads were e-beam evaporated onto the 100 nm SiO₂ gate dielectric. The back gate consists of 100 nm thick gold evaporated on the back of the n⁺ silicon substrate. The molecular structure of CuPc, CoPc, and H₂Pc is shown on the right.

density of trap states due to either the structural or electrical defects.²³ Charge trapping at these states occurs over a large time scale, ranging from seconds to hours. The kinetics of trapping depends on film structure,¹⁶ electrical field,¹⁵ and gate dielectric surface treatments.²⁴ Therefore, the BSE related baseline drift of ChemFETs cannot be solved by applying a simple baseline compensation method.

In this report, a pulsed gating method has been shown to greatly reduce the charge trapping effect in ChemFETs. The method effectively eliminates the baseline drift in OTFTs made of three different channel materials and three channel thicknesses over a 20 h period. On exposure to volatile organic vapor pulses, the chemical response under pulsed gating is completely reversible with a baseline variation less than 0.1%/h. It is suggested that the intrinsic trap states rather than analyte-induced traps are the major sources of baseline instability in ChemFETs when the analyte exhibits reversible absorption. The ultralow drift operating technique obviates the need to employ complicated drift compensation techniques¹¹ and may enable more robust e-nose systems.

II. EXPERIMENT

The organic channel materials used in this work were metal phthalocyanines with copper or cobalt metal centers (CuPc or CoPc) and the metal-free phthalocyanine (H₂Pc). The phthalocyanines are known to have high chemical sensitivity and selectivity to organic vapors.^{25–27} The thicknesses of the organic thin films were between 4–50 ML (ML denotes monolayer). CuPc, CoPc, and H₂Pc materials were purchased from Aldrich and purified three times by zone sublimation. Bottom-contact devices were fabricated on n⁺ silicon wafers with 100 nm of thermally grown SiO₂. Gold was evaporated onto the back of the silicon wafers to form the gate electrode. The channel length and width of the devices were 10 μm and 2 mm, respectively, defined by a photolithography process. Interdigitated electrodes with 25 pairs of fingers were used to increase the output current. A schematic cross section of a ChemFET and the molecular structure of the sensing materials are shown in Fig. 1.

CuPc, CoPc, and H₂Pc films were deposited by organic molecular beam epitaxy at 80 °C at rates between 0.4 and 1 Å/s. The films were 20 ML CuPc, 4 ML CoPc, 50 ML

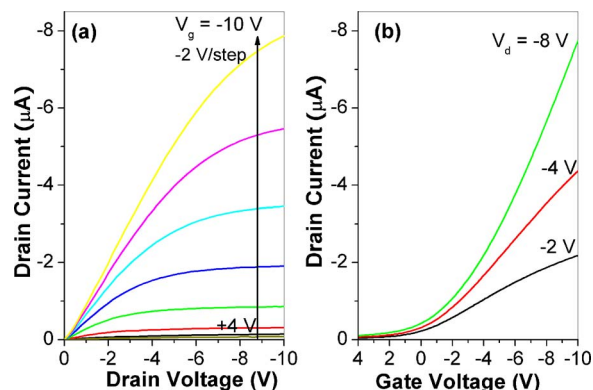


FIG. 2. (Color online) Output (a) and transfer (b) characteristics of a typical ChemFET (50 ML CoPc).

CoPc, and 25 ML H₂Pc. The film thicknesses were measured by a quartz crystal microbalance during deposition, and calibrated by atomic force microscopy and x-ray diffraction measurements. The *d* spacing is 13.3 Å in accordance with previous measurements that show that the phthalocyanine molecules are oriented perpendicular to the substrate surface.^{10,28} Six duplicate ChemFETs were deposited for each device under investigation. No annealing was performed on the deposited devices, but all devices were exposed to air for at least one month prior to use to ensure repeatable chemical responses in air. The six devices had only 5% variation in electrical conductivity and chemical sensing response. We have not studied the variation between devices deposited on different substrates since that would require very tight control over our process conditions. A typical output and the transfer characteristics of an OTFT sensor are shown in Fig. 2. All the devices were p-channel transistors and had threshold voltages between -0.38 and +0.38 V. The mobility values extracted in linear regions are between 2.0 × 10⁻⁵ and 2.6 × 10⁻⁴ cm²/V s.

The electrical properties of the devices were measured using a Keithley 6385 picoammeter and programmable Agilent E3631A power supply. The electrical measurement system was calibrated with a HP 4156B precision semiconductor parameter analyzer. For the pulsed measurement at different frequencies, a homebuilt transient spectroscopy system has been developed utilizing National Instrument's 6040E DAQPad and a FEMTO DLPCA-200 variable gain low-noise current amplifier. The transient spectroscopy system was also calibrated with the HP 4156B parameters analyzer.

Chemical sensing experiments were carried out inside a custom built flow system controlled by a computer. The devices were loaded inside the optically isolated chamber under dry air flow for two days before testing to eliminate photocurrents and doping by H₂O, O₃, and other ambient reactive trace gases. The temperature in the chamber was kept at 27 ± 0.2 °C using a Haake constant temperature bath. Bubblers filled with liquid analyte were kept in a water bath chilled to 15 °C. Mass flow controllers were used to dilute and introduce analyte vapors at a known concentration into a manifold, where they were premixed and diluted with the carrier gas before introduction into the test chamber. Sole-

noid valves before and after the analyte bubblers were used to prevent cross contamination between analytes. A four-way valve was used to minimize the dead time between the introduction of each analyte pulse. The analytes employed were methanol, diisopropyl methylphosphonate (DIMP), and dimethyl methylphosphonate (DMMP) at a constant flow rate in dry air. All the devices have been found to have stable output characteristics for one year after fabrication. However, the electrical noise of all the ChemFET devices increases after one month of intense testing. The increase in noise was more severe for the thinner devices and was consistently observed for all the thin devices. Replacing the cables or resoldering the leads to the contact pads did not reduce the increased noise. The results indicate that the electrical noise may be due to the aging of contacts between organic films and metal electrodes.

III. RESULTS AND DISCUSSION

In the first part of the report, we refined the gate pulsing technique to eliminate baseline drift in the CuPc ChemFETs without chemical analytes. Using relatively short test periods (2 h), the effect of the gate duty cycle on the baseline stability was measured as a function of gate duty cycle and frequency to find an optimized operating condition. Subsequently, the optimal pulse cycle was applied over a testing period of 20 h to measure the long term baseline stability. We have tested the pulsed gating in the absence of analyte on ChemFETs made of two other phthalocyanine materials to demonstrate that the pulsed gating method generally improves electrical stability of ChemFETs.

In the second part of the report, the impact of BSE on CuPc ChemFET baseline stability was quantified by comparing chemical responses to methanol vapor pulses under static and pulsed gating. The statistics of BSE effect in drift and chemical sensitivity was obtained from 15 identical methanol pulses.

In the third part of this report, the pulsed gating method was applied for ChemFET detection of low vapor pressure organophosphonate nerve agent simulants. The analyte pulse duty cycle has been varied to separate analyte-induced baseline drift from electrical-induced drift. Given sufficient time to allow analytes desorption from the film, the baseline drift to these analytes can also be reduced to negligible levels.

A. Optimal gate pulse selection

To better understand and control the electrical stability of ChemFETs, the drain current was measured over 2 h in the absence of analytes. The CuPc ChemFET devices were loaded in the chamber for two days and fully relaxed from bias stress. Gate pulse trains of 0.1 Hz were applied at the gate electrode between duty cycles of 1%–100%. The “on” gate voltage was fixed at -8 V, while the “off” gate voltage was fixed at 0 V. Shown in Fig. 3(a) are the drain currents normalized to the initial current in each measurement. We found that under static gate bias (100% gate duty cycle), the baseline drifted 25% after 2 h. The baseline drift with 1% gate duty cycle was less than 0.1% over 2 h, which is 250 times less than under the static gate bias. During the tests, the

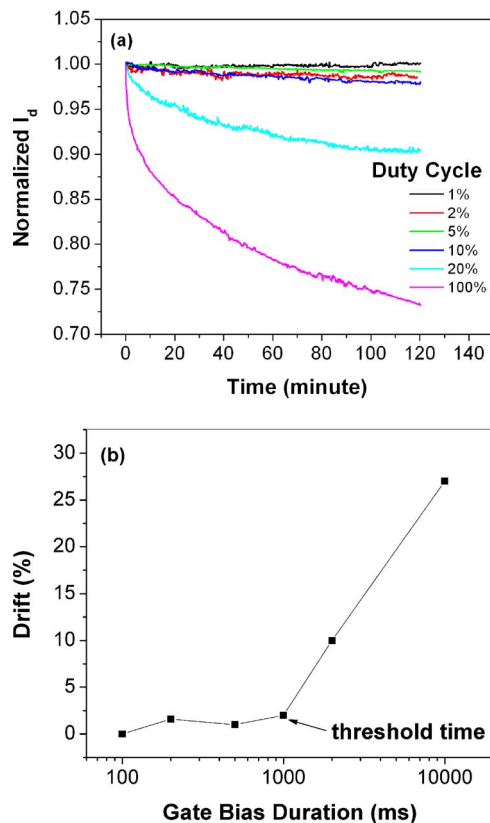


FIG. 3. (Color online) ChemFET baseline study in the absence of analytes (20 ML CuPc). (a) Normalized drain current for 0.1 Hz gate pulses (V_g from 0 to -8 V) with duty cycles between 1% and 100%. The drain voltage is held constant at -4 V. (b) The baseline drift vs pulse duration.

drain voltage was held at constant (-4 V). We did not observe baseline drift at low gate duty cycle. Therefore, bias stress due to static drain bias can be excluded as a cause of BSE in these devices.

The percentage baseline drift as a function of the pulse duration was calculated from data in Fig. 1(a) and is shown in Fig. 3(b). For 0.1 Hz gate pulses, the baseline drift over 2 h rose above 1% only for pulse durations greater than 1 s. We have also measured the baseline drift at constant pulse duration (100 ms) while varying the frequency of the pulses between 0.05 and 5 Hz. We found that the baseline drift in 2 h rose above 1% for pulse frequencies above 1 Hz. Further reducing the pulse duration to keep the duty cycle constant increases the noise. Therefore, in all the measurements, the pulse frequency was held at 0.1 Hz.

To test the feasibility of the pulsed gating method for continuous operation of ChemFETs, we compared the baseline stability of the devices over a period of 20 h. The drain current has been measured with a -8 V gate voltage pulsed at 0.1 Hz (1% duty cycle) and contrasted with results for a -8 V static gate and a -4 V static gate. The baseline drift was found to be less than 1% over 20 h with pulsed gating, as shown in Fig. 4. Conversely, the baseline drift was 55% over 20 h for a static gate bias at -8 V. The BSE has been reported to depend on gate bias in amorphous silicon TFTs.²⁹ Reducing the static gate bias by half to -4 V only reduced the drift with the static gate from 55% to 38% over 20 h. The

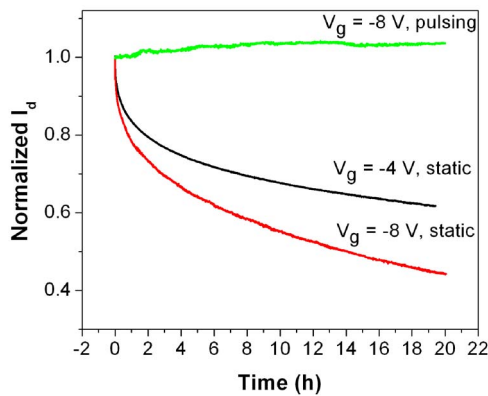


FIG. 4. (Color online) The baseline stability for ChemFETs (20 ML CuPc) over 20 h for 0.1 Hz, 1% duty cycle ($V_g = -8$ V), and pulsed gate vs static gate bias at -4 and -8 V. Gate voltage was varied to show no dramatic decrease in drift under static bias condition.

results indicate that the baseline drift problem can only be effectively solved by the pulsed gating method.

To prove that the pulsed gating method is of general utility for ChemFETs and not exclusive to CuPc devices, the pulsed gate operation was tested on CoPc and H₂Pc ChemFETs. The baselines measured over 20 h using the 0.1 Hz gate pulses are shown in Fig. 5. The same gate pulse train (0.1 Hz, 1% duty cycle, -8 V) employed for the 20 ML CuPc ChemFET was applied in the measurements. For channels of all three materials and for all channel thicknesses tested (4–50 ML), the pulsed gating operation reduced the baseline drift below 0.1% /h. In all the above measurements, the rest gate voltage was set at 0 V, which is within 0.5 V of the threshold voltages for all the above devices. The threshold voltages of the 50 and 4 ML CoPc ChemFETs are -0.38 and $+0.38$ V, respectively. We note that the 0 V rest voltage causes a positive drift in the 50 ML CoPc ChemFET, while a negative drift occurs in the 4 ML CoPc ChemFET (see Fig. 5). For devices with nonzero threshold voltage, we found that the rest gate voltage needs to be set close to the threshold voltage to minimize the bias stress. To demonstrate that the sign of the baseline drift is controlled by the offset between the rest voltage and the threshold voltage, we tested a device with nonzero threshold voltage ($+1.3$ V) at three dif-

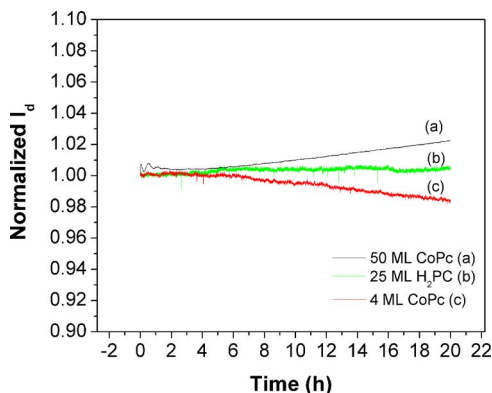
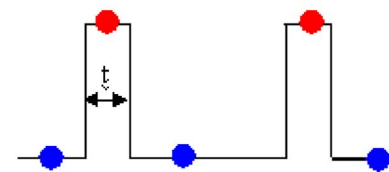
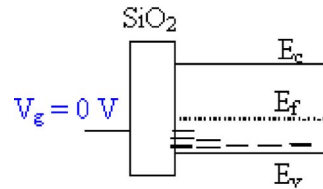


FIG. 5. (Color online) Pulsed gating operation (0.1 Hz, 1% duty cycle, -8 V) of ChemFETs with three different channel materials/thicknesses over 20 h: (a) 50 ML CoPc, (b) 25 ML H₂Pc, and (c) 4 ML CoPc.

Gate pulse train



“Off-state”



“On-state”

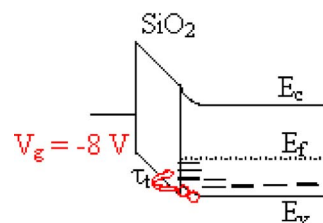


FIG. 6. (Color online) Energy band diagrams of OTFT response to gate pulses. The band diagrams of the “off” and “on” states of OTFTs are shown at different voltages. Break lines represent trap states located near the SiO₂ interface and in the bulk. At on states, the accumulated holes are trapped by trap states at a finite capture time “ τ_t .”

ferent rest voltages. The rest voltage at $+2$ V induced positive drift, while the rest voltage at 0 V induced negative drift (see EPAPS document).³⁰

The baseline drift under static gate bias in OTFTs has been attributed to the threshold voltage shift over time induced by a slow charge trapping process.¹⁵ Trap states are distributed both near the gate dielectrics and in the bulk films in OTFTs. Trapping and detrapping processes occur simultaneously in OTFTs. The device response to gate pulses can be qualitatively explained by an energy band diagram model shown in Fig. 6. At 0 V gate bias, the device is assumed to rest in flat band condition. There is no charge accumulation in the channel at this bias condition. The flat band voltage depends on the threshold voltage of the devices, which is 0 V for the device in Fig. 6. Conversely, at -8 V, hole carriers are accumulated in the channel by the gate capacitor. Carriers are trapped in states within the band gap at different rates depending on the capture cross section of trap states.³¹ For gate bias pulses between 0 and -8 V, the above device goes between flat band and accumulation conditions. There is a finite charge trapping time τ_t for the trap states to capture holes. We hypothesize that if the gate stress time t is less than τ_t , the charge trapping effect can be greatly reduced. The phenomenon was observed on all devices that were tested. The results shown in Fig. 3(b) are consistent with a charge trapping time between 1 and 2 s in the 20 ML CuPc ChemFETs.

To confirm that the bias stress is a charge trapping process in the organic channel instead of in the gate oxide, the

change in output current versus time is analyzed. The time dependence of electrical instability in amorphous silicon and organic thin-film transistors has been investigated in detail.²⁹ The kinetics of BSE is usually modeled from the time dependent threshold voltage shift. The evolution of threshold voltage in the 20 ML CuPc ChemFET can be calculated from the time dependent drain current shown in Fig. 4. In the linear region, the drain current of OTFT is

$$I_d = \frac{W}{L} C_i \mu (V_g - V_t) V_d, \quad (1)$$

where C_i is the gate capacitor, W and L are the transistor width and length, and μ is the effective field-effect mobility. The mobility has been found to be constant during the bias stress experiments.²¹ Based on the above assumption, the threshold voltage shift can be deduced from the drain current as follows:

$$V_t(t) = V_{t0} - [I_d(t) - I_{d0}] \left/ \left(\frac{W}{L} C_i \mu V_d \right) \right., \quad (2)$$

where V_{t0} and I_{d0} are the initial threshold voltage and drain current. The kinetics of BSE at $V_g = -8$ V has been fitted with a power law dependent function,

$$\Delta V_t = -0.333(t)^{0.32},$$

$$\text{with } R^2 = 0.9999. \quad (3)$$

Similarly, the BSE at $V_g = -4$ V can be well fitted by the power law with a power coefficient 0.27. On amorphous silicon TFTs, it has been experimentally found that charge trapping in the gate dielectrics follows logarithmic kinetics, while charge trapping in the a -Si channel follows the power law kinetics.²⁹ Our bias stress has a power law dependence and a time scale consistent with the charge trapping effect in the organic channel.

B. Baseline drift with high volatility analyte

The baseline stability of the 20 ML CuPc ChemFETs in the presence of high volatility analytes has been investigated. Highly volatile analytes were employed to ensure that the chemically induced drift due to accumulation of analyte by the organic film is negligible and that all drift is due to electrical instability. Shown in Fig. 7 is a comparison between static and pulsed gating operations of the ChemFETs exposed to 15 methanol chemical pulses. Each chemical pulse was 20 min long followed by 1 h recovery. With 1% duty cycle, 0.1 Hz gate pulsing at -8 V, the chemical response was found to be fully reversible. The mean baseline drift value is calculated by measuring the accumulated drift for each of the 15 pulses referenced to the same starting point. The baseline drift was $(0.09 \pm 0.016) \%$ /h within the 20 h test duration, which is comparable within a factor of 2 to the rate of drift observed in the absence of analyte. Similar ultralow baseline drift to methanol pulses has been found with the CoPc and H₂Pc ChemFETs. Conversely, with a static gate bias, the baseline drifted over 60% during 20 h of

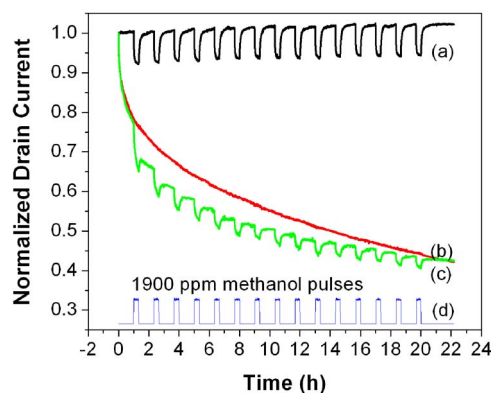


FIG. 7. (Color online) ChemFET baseline study in the presence of methanol in dry air (20 ML CuPc). (a) 0.1 Hz, 1% duty cycle gate bias with methanol exposure, (b) static bias with methanol exposure, (c) static bias without methanol exposure, and (d) 1900 ppm methanol pulses.

methanol pulsing. A control experiment of baseline drift due to bias stress in the absence of analyte is also shown in Fig. 7.

At a macroscopic level, the chemical response of OTFTs can be attributed to changes in threshold voltage and mobility values. BSE also causes the threshold voltage shift, and therefore, impairs the chemical sensing properties of the ChemFETs. For the 1% duty cycle, 0.1 Hz pulsed gating, the chemical sensitivity to methanol is $4.05 \pm 0.03 \times 10^{-3} \%$ /ppm. For static gate operation, the chemical sensitivity is $(2.10 \pm 0.28) \times 10^{-3} \%$ /ppm after correcting for baseline drift. Bias stress increased the standard error in chemical sensitivity measurements by a factor of 10. The increased chemical sensitivity uncertainty with static gate bias is due to the nonlinear behavior of the bias stress effect. Even though the baseline of ChemFETs in the absence of analytes is highly repeatable, and can be well fitted with the power law, the exposure to analyte changes the kinetics, which cannot be accurately modeled.

C. Baseline drift with low volatility analytes

For low volatility analytes, such as nerve gas simulants, it is important to separate the electrical and chemical sources of baseline drift. The 20 ML CuPc ChemFET was employed for detecting nerve gas simulants using the 1% duty cycle, 0.1 Hz at -8 V gate pulsing. The chemical responses to 15 pulses of 19 ppm DIMP (simulant for Soman) and 32 ppm DMMP (simulant for Sarin) are shown in Fig. 8. The chemical sensitivity to DIMP is $(327.5 \pm 11.79) \times 10^{-3} \%$ /ppm with a drift of $(1.15 \pm 0.73) \%$ /h. The chemical sensitivity to DMMP is $(178.7 \pm 4.9) \times 10^{-3} \%$ /ppm with a drift of $(0.45 \pm 0.1) \%$ /h. The drifts for DIMP and DMMP are 12 and five times larger as compared to methanol using the same testing protocol. We note that the recovery process of methanol and DIMP pulses can be fitted with exponential decays. The decay time scales are approximately three times larger for DIMP as compared to methanol, indicating that the binding energy between DIMP and CuPc is approximately $\log(3)$ times larger as compared to the binding energy be-

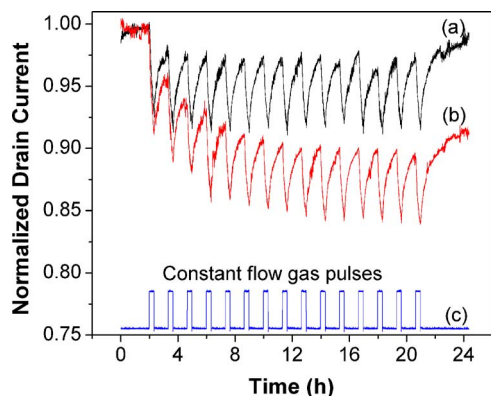


FIG. 8. (Color online) ChemFET (20 ML CuPc) responses to nerve gas simulants in dry air (0.1 Hz, 1% duty cycle, -8 V gate pulse train): (a) chemical response to DMMP (32 ppm), (b) chemical response to DIMP (19 ppm), and (c) analyte gas pulses, 20 min long followed by 60 min recovery.

tween methanol and CuPc. Therefore, the large baseline drift to DIMP in the above testing protocol may be due to insufficient time for DIMP desorption.

To prove that the increase drift for DIMP and DMMP is due to purely analyte-induced drift, the chemical responses to DIMP pulses were recorded as a function of the recovery time. A longer recovery time allows a low vapor pressure analyte sufficient time to desorb from the ChemFET thereby reducing the analyte-induced drift. Shown in Fig. 9 are the chemical responses with the same dosage but using different recovery times. It has been found that the drift to DIMP doses is reduced by 30 times to $(0.036 \pm 0.007) \%$ /h when the recovery time is increased to 3 h. Therefore, the increased drift in the presence of high boiling point analytes should be ascribed to analyte-induced drift from accumulation of analyte in the film during the time scale of the experiment. This study shows that by combining a low duty cycle analyte dose with a low duty cycle pulsed gating, the baseline drift for low vapor pressure analytes can be reduced to a level similar to those attained for highly volatile analytes.

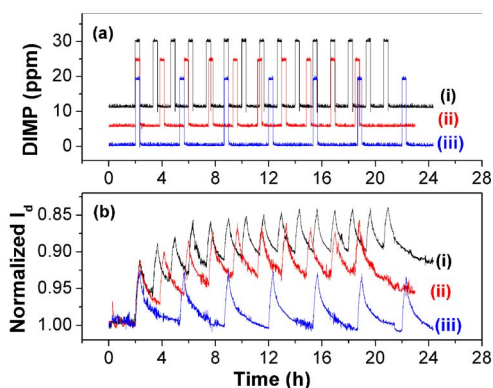


FIG. 9. (Color online) ChemFET (20 ML CuPc) response to DIMP pulses using different recovery times in dry air with 1% duty cycle, 0.1 Hz at -8 V gate pulsing: (a) 20 min DIMP pulses with 60 min (i), 90 min (ii), and 180 min (iii) recovery times. The concentration has been offset by 10 and 5 ppm for (i) and (ii). (b) Chemical response to the DIMP pulses shown in (a).

IV. CONCLUSION

The impact of the bias stress effect on the baseline stability of ChemFETs has been investigated. Under static gate bias, a nonlinear baseline at an average rate of 2.5% /h has been observed in CuPc ChemFETs exposed to methanol dosing pulses. By pulsing the gate voltage at 0.1 Hz with a 1% duty cycle, the baseline drift has been reduced to 0.09% /h. The pulsed gating method also decreases the uncertainty in chemical sensing by an order of magnitude. The pulsed gating method has been found to be generally applicable for ChemFETs made from two other materials, and for low vapor pressure nerve gas simulants when sufficient time is allowed for complete analyte desorption from the film. It is concluded that OTFT chemical sensors can be used as low drift sensing elements in e-noses, utilizing the pulsed gate techniques.

ACKNOWLEDGMENTS

One of the authors (R.D.Y.) thanks Byron Ho and Vincent So for the assistance with sensing instrument developments. Funding from AFOSR MURI (No. F49620-02-1-0288) and NSF (No. CHE-0350571) is acknowledged.

- ¹L. Torsi, A. Dodabalapur, L. Sabbatini, and P. G. Zamboni, *Sens. Actuators B* **67**, 312 (2000).
- ²E. S. Kolesar and J. M. Wiseman, *Anal. Chem.* **61**, 2355 (1989).
- ³B. Crone, A. Dodabalapur, A. Gelperin, L. Torsi, H. E. Katz, A. J. Lovinger, and Z. Bao, *Appl. Phys. Lett.* **78**, 2229 (2001).
- ⁴Z. T. Zhu, J. T. Mason, R. Dieckmann, and G. G. Malliaras, *Appl. Phys. Lett.* **81**, 4643 (2002).
- ⁵T. Someya, H. E. Katz, A. Gelperin, A. J. Lovinger, and A. Dodabalapur, *Appl. Phys. Lett.* **81**, 3079 (2002).
- ⁶L. Wang, D. Fine, and A. Dodabalapur, *Appl. Phys. Lett.* **85**, 6386 (2004).
- ⁷F. Liao, C. Chen, and V. Subramanian, *Sens. Actuators B* **107**, 849 (2005).
- ⁸J. B. Chang, V. Liu, V. Subramanian, K. Sivula, C. Luscombe, A. Murphy, J. S. Liu, and J. M. J. Frechet, *J. Appl. Phys.* **100**, 014506 (2006).
- ⁹M. Bouvet, G. Guillaud, A. Leroy, A. Maillard, S. Spirkovitch, and F. G. Tournilhac, *Sens. Actuators B* **73**, 63 (2001).
- ¹⁰R. D. Yang, T. Gredig, J. Park, C. Colesniuc, I. K. Schuller, W. C. Trogler, and A. C. Kummel, *Appl. Phys. Lett.* **90**, 263506 (2007).
- ¹¹T. C. Pearce, S. S. Schiffman, H. T. Nagle, and J. W. Gardner, *Handbook of Machine Olfaction* (Wiley-VCH, Weinheim, 2003).
- ¹²S. V. Patel, T. E. Mlsna, B. Fruhberger, E. Klaassen, S. Cemalovic, and D. R. Baselt, *Sens. Actuators B* **96**, 541 (2003).
- ¹³H. E. Katz, *Electroanalysis* **16**, 1837 (2004).
- ¹⁴L. Torsi and A. Dodabalapur, *Anal. Chem.* **77**, 380A (2005).
- ¹⁵S. J. Zilker, C. Detcheverry, E. Cantatore, and D. M. de Leeuw, *Appl. Phys. Lett.* **79**, 1124 (2001).
- ¹⁶H. L. Gomes *et al.*, *Appl. Phys. Lett.* **84**, 3184 (2004).
- ¹⁷G. Horowitz, M. E. Hajlaoui, and R. Hajlaoui, *J. Appl. Phys.* **87**, 4456 (2000).
- ¹⁸R. J. Chesterfield, J. C. McKeen, C. R. Newman, C. D. Frisbie, P. C. Ewbank, K. R. Mann, and L. L. Miller, *J. Appl. Phys.* **95**, 6396 (2004).
- ¹⁹T. Minari, T. Nemoto, and S. Isoda, *J. Appl. Phys.* **99**, 034506 (2006).
- ²⁰S. Jung, T. Ji, and V. K. Varadan, *Appl. Phys. Lett.* **90**, 062105 (2007).
- ²¹A. Salleo and R. A. Street, *J. Appl. Phys.* **94**, 471 (2003).
- ²²J. B. Chang and V. Subramanian, *Appl. Phys. Lett.* **88**, 233513 (2006).
- ²³R. Schmechel and H. von Seggern, *Phys. Status Solidi A* **201**, 1215 (2004).
- ²⁴C. Goldmann, C. Krellner, K. P. Pernstich, S. Haas, D. J. Gundlach, and B. Batlogg, *J. Appl. Phys.* **99**, 034507 (2006).
- ²⁵A. W. Snow and W. R. Barger, *Phthalocyanines Properties and Applications* (Wiley, New York, 1989).
- ²⁶R. Zhou, F. Josse, W. Gopel, Z. Z. Ozturk, and O. Bekaroglu, *Appl. Organomet. Chem.* **10**, 557 (1996).
- ²⁷J. D. Wright, *Prog. Surf. Sci.* **31**, 1 (1989).
- ²⁸C. W. Miller, A. Sharoni, G. Liu, C. N. Colesniuc, B. Fruhberger, and I. K.

Schuller, Phys. Rev. B **72**, 104113 (2005).

²⁹M. J. Powell, C. Vanberkel, and J. R. Hughes, Appl. Phys. Lett. **54**, 1323 (1989).

³⁰See EPAPS Document No. E-JAPIAU-102-125715 for the comparison of baseline drift on CoPc ChemFET with different rest voltages. This docu-

ment can be reached via a direct link in the online article's HTML reference section or via the EPAPS homepage (<http://www.aip.org/pubservs/epaps.html>).

³¹D. K. Schroder, *Semiconductor Material and Device Characterization* (Wiley, New York, 1998).